Light Streak Tracking of Optically Trapped Thin Microdisks

Z. Cheng,[1,*] P. M. Chaikin,[1,2] and T. G. Mason[1]

[1]*Corporate Strategic Research, ExxonMobil Research and Engineering Company, Route 22 East, Annandale, New Jersey 08801*
[2]*Princeton University, Department of Physics, Jadwin Hall, Princeton, New Jersey 08544*

(Received 4 February 2002; published 19 August 2002)

Nonspherical particles can uniquely probe soft system dynamics. We show that laser tweezers stably trap thin coinlike microdisks in 3D with an edge-on orientation. Scattered light forms a streak that we track using a fast camera to measure the disk's angular displacement. Linearly polarized tweezers rotationally trap a birefringent disk, and we measure its harmonically bound Brownian rotation over 5 decades in time. Near a surface, the disk exhibits a translational-orientational switchback oscillation. Circularly polarized tweezers rotate the disk and streak, yielding a colloidal lighthouse.

DOI: 10.1103/PhysRevLett.89.108303 PACS numbers: 82.70.–y, 05.40.–a, 42.62.–b, 78.35.+c

Laser tweezers [1–3] are commonly used to trap and manipulate microspheres in three dimensions, yet their utility for trapping and manipulating nonspherical microparticles remains incomplete due to the additional geometrical complexity. Optical trapping of long cylinders with their symmetry axes along the laser beam has been previously predicted [4] and observed [5]. However, for short coinlike cylinders, the same theoretical model predicts that tweezers cannot trap disks having radii and thicknesses much greater than the wavelength of light stably in 3D [4]. Likewise, light scattered by trapped microspheres has been studied [6,7], but it has not been considered for less symmetric microparticles that have dimensions near or below the wavelength of visible light. The interaction between light and asymmetric dielectric particles is of widespread importance, since many naturally occurring particles that could be tweezed are not spherical.

We approach this issue by applying laser tweezers to coinlike wax microdisks and to lithographically prepared polymethylmethacrylate (PMMA) microdisks having a typical diameter-to-thickness aspect ratio, ρ, of about five. Despite a calculation that suggests that tweezed microdisks cannot satisfy force and torque equilibria simultaneously [4], we are able to trap thin microdisks having a wide range of radii in 3D. These ''thin'' disks have thicknesses comparable to or less than the beam waist at the focus of the tweezer (i.e., near the wavelength of light); this thickness regime lies below that of the calculation. When trapped, a thin disk orients with its symmetry axis perpendicular to the beam. This orientation causes the backscattered laser light to form a streak parallel with the disk's faces, yielding a natural optical lever for sensing rotation. By exploiting this optical lever, we introduce a novel high-speed scattering technique, light streak tracking (LST), for precisely measuring rotational fluctuations of a single microdisk. The wax disks are birefringent, whereas the PMMA disks are not. This allows us to separate the effects due to structural and optical anisotropies. In particular, we find that the PMMA disks rotate freely in linearly polarized (LP) light, whereas the wax disks are rotationally bound. Using high-speed digital imaging of the scattered streak, we have precisely measured the mean square angular displacement of a rotational harmonically bound Brownian wax microdisk in a LP tweezer. A birefringent disk trapped in a circularly polarized (CP) tweezer rotates, and its light streak creates a colloidal lighthouse. Finally, LP-trapped microdisks near a wall exhibit a coupled translational-orientational ''switchback'' oscillation. Unless otherwise noted, the following discussion relates to the birefringent wax microdisks.

We make microdisks by shear emulsifying hot α-eicosene wax [CH_3—$(CH_2)_{17}$—$CH{=}CH_2$] at 80 °C in a concentrated aqueous solution of sodium dodecyl sulfate (SDS). This emulsion is diluted and cooled to room temperature below the bulk eicosene melting temperature [8]: $T_m = 26.2$ °C. After several weeks, microscope observations reveal about 5% thin micron-sized coinlike wax disks with radii, a, of $0.2\ \mu\text{m} < a < 10\ \mu\text{m}$ and $2 < \rho < 10$ ($\rho = 5$, typically) among mostly spherical particles. We speculate that the right circular cylindrical structure of the disks arises when the cooled wax enters a lamellar liquid crystalline rotator phase that occurs at 29.8 °C. The lamellar planes lie parallel to the flat edges, and the in-plane orientational disorder of wax molecules facilitates an in-plane isotropic surface energy that permits a circular perimeter. Attractive depletion forces [9], induced by raising the SDS concentration to create micelles, are repeatedly used to segregate the disks. The shape selectivity arises because two disks oriented face-to-face create a much larger excluded volume than a disk-sphere combination. Under differential interference contrast microscopy, the disks appear to be birefringent, as shown in Fig. 1(a).

The laser tweezers consist of an inverted microscope with an expanded laser beam that enters the microscope through the epifluorescence port and is reflected upward into the 100× 1.4 NA oil-immersion objective by a dichroic mirror. Green illumination passes down through the condenser lens. We use either a He-Ne laser at a wavelength of $\lambda = 633$ nm and power of $P = 15$ mW, or, for additional power, a solid state Nd:YAG laser at

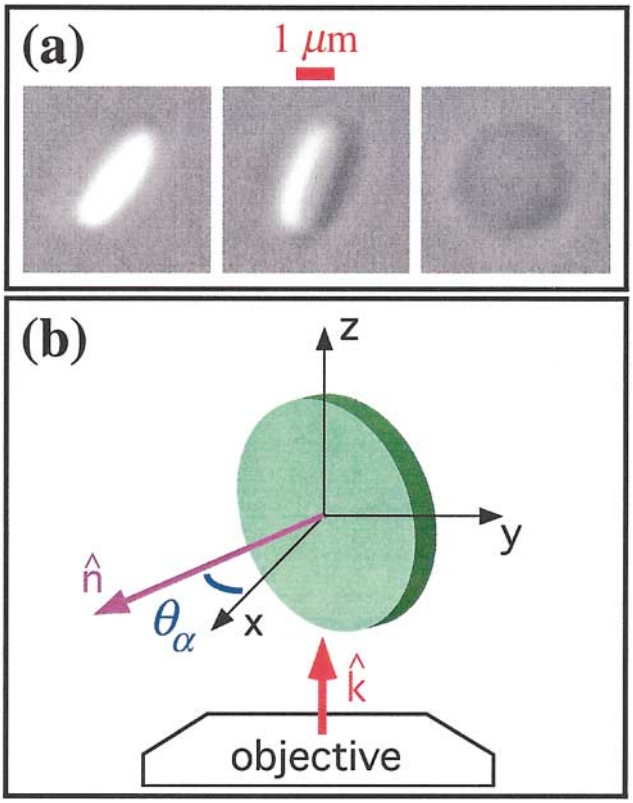

FIG. 1 (color). (a) Optical micrographs of a wax microdisk suspended in water as it undergoes rotational diffusion. (b) Tweezing a microdisk. The propagation direction, $\hat{k}$, of the laser beam is in the z direction. The tweezed disk aligns edge-on with its symmetry axis, $\hat{n}$, perpendicular to $\hat{k}$. The angular displacement, θ_α, fluctuates due to Brownian thermal forces.

$\lambda = 1064$ nm and $P = 10$ W; both lasers are LP. Strikingly, all disks are trapped stably in 3D, regardless of radius or aspect ratio even for those approaching the microscope's resolution limit of 0.2 μm. They align edge-on with their symmetry axes perpendicular to the beam axis, thereby maximizing the disk's volume in the region of highest electric field, as shown pictorially in Fig. 1(b). The LP tweezer creates a harmonic restoring torque that causes the disk's symmetry axis to lie perpendicular to the polarization direction [10–12]. By changing the polarization direction, the in-plane orientation of its symmetry axis can be controlled. Disks can be manipulated in the z direction without disturbing their orientation by adjusting the focus. Thermal fluctuations cause higher amplitude translational excursions of the center of the disk along its edge as compared to its symmetry axis. For small P at which the disk is barely trapped translationally, the disk exhibits rocking orientational fluctuations, causing its symmetry axis to deviate from the focal plane.

The anisotropic shape of the trapped disk profoundly alters the light emanating from the focal region. Diffraction of the tightly focused beam by the thin dielectric plate leads to a streak of forward-scattered light along the disk's symmetry axis. The high emergence angle of this light streak creates a natural optical lever that is extremely sensitive to the disk's orientation. Some of the incident focused beam is refracted back through the objective by the disk's circular edge and is collected by the objective, yielding a light streak oriented perpendicular to the disk's symmetry axis, as in Fig. 2(a) (inset).

We exploit this natural optical lever to study the rotational diffusion of a single microdisk in a torque trap, determining its orientation using LST. A high-speed digital camera (Kodak Motion Corder SR-Ultra) records movies of the light streak's deflections. The intensity profile of the streak away from the reflected beam is fit to a straight line (Research Systems IDL), yielding time traces of the angular displacement of the disk's symmetry axis, θ_α, with 10 μs temporal resolution and 1 mrad angular resolution,

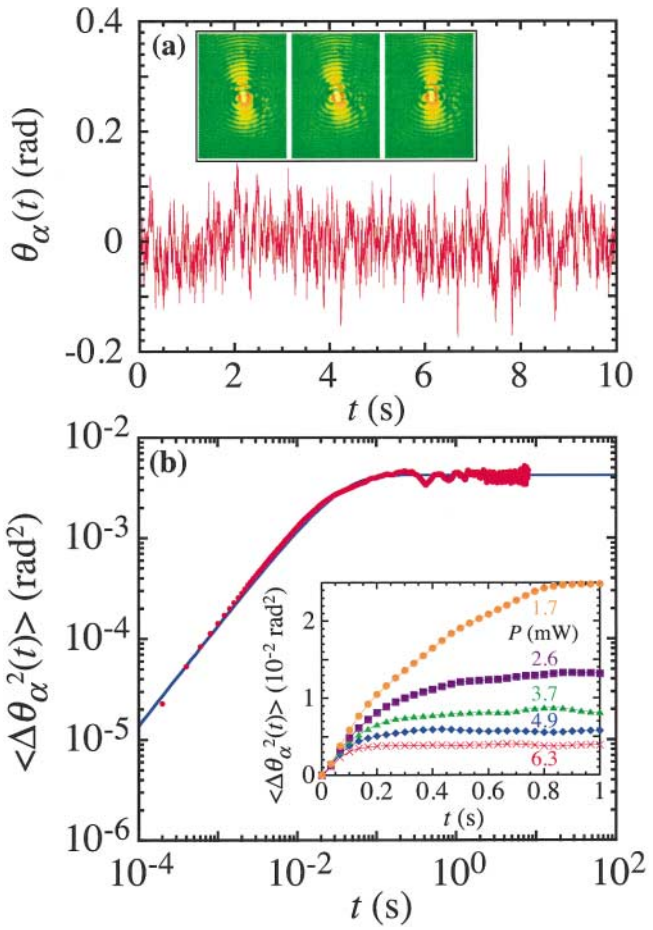

FIG. 2 (color). (a) The time-dependent angular displacement, $\theta_\alpha(t)$, of a wax microdisk (radius 1.2 μm) in a rotational trap created by a LP laser tweezer at a power of $P = 6.3$ mW, measured by imaging the streak of red laser light collected by the objective lens using the high-speed camera at 5000 frames/s over a duration of 10 s. Inset: Micrographs of a wax disk in a rotational harmonic trap separated by 1/6 s. The backscattered light forms a streak in the plane normal to the viewing direction. (b) The time-averaged mean square angular displacement $\langle \Delta\theta_\alpha^2(t) \rangle$ (points) determined from (a). The solid line is a fit using Eq. (2). Inset: $\langle \Delta\theta_\alpha^2(t) \rangle$ measured using light streak tracking (LST) of the red channel of the color CCD at 30 Hz for a series of different He-Ne laser powers, P.

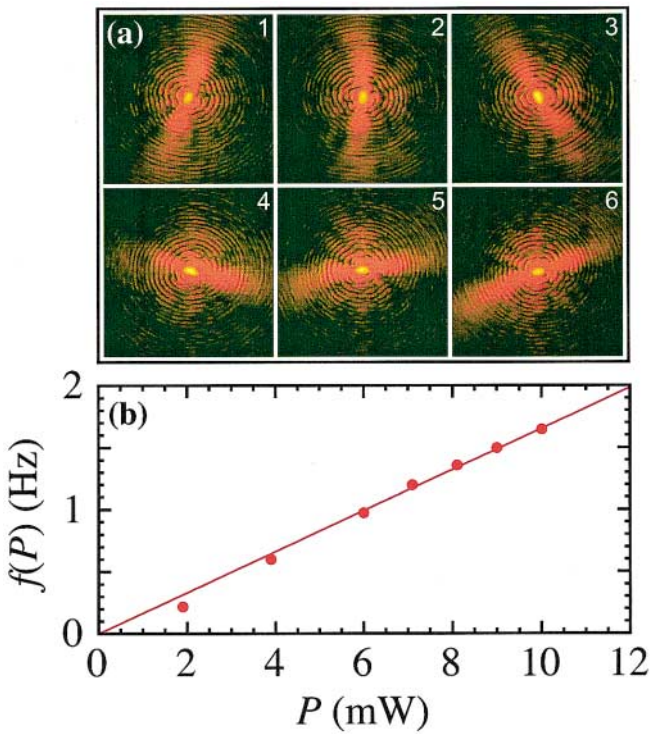

FIG. 3 (color). (a) Colloidal lighthouse created by rotation of the red light streak from a trapped wax microdisk (radius 1.5 μm) using a CP laser tweezer ($P = 10$ mW). The counterclockwise rotation of the streak is shown in successive micrographs (1–6) separated by 1/6 s. (b) The rotational frequency, f, as a function of laser power, P (solid circles) increases linearly, as shown by the fit (solid line).

as shown in Fig. 2(a). The rapid fluctuations in θ_α reflect the random thermal torque that drives the rotational diffusion, yet the LP light interacts with the birefringent wax to create a restoring torque that restricts the diffusion over long times, causing θ_α to be bounded. The time averaged $\langle \Delta\theta_\alpha^2(t)\rangle$ is shown in Fig. 2(b). This is the first measurement of the rotational harmonically bound Brownian particle that captures both the short time diffusion and the long time saturation due to the orientational trap. Additional LST measurements with the slower 30 Hz color CCD camera show that the saturation value of $\langle \Delta\theta_\alpha^2\rangle$ varies inversely with the laser power [see Fig. 2(b) (inset)].

The disk's orientational fluctuations can be described by a Langevin torque equation including a white-noise thermal driving torque τ_R, a viscous drag torque, and an optical restoring torque [11,12]:

$$I\ddot{\theta}_\alpha = \tau_R - \zeta\dot{\theta}_\alpha - \frac{P_{\text{eff}}}{\omega_o}\sin(R)\sin(2\theta_\alpha), \qquad (1)$$

where I is the rotational inertia of the disk about its edge, ζ is the rotational viscous friction factor, P_{eff} is the effective power of the laser light that interacts with the disk (proportional to but less than P), ω_o is the optical frequency, and R is the effective average retardation of the light as it traverses the disk. Perrin's calculation for an oblate ellipsoid [13] gives $\zeta \approx 8\pi\eta a^3 H(\rho)$, where η is the viscosity and $H(\rho) > 1$. The retardation is $R \approx 4\pi\Delta n a/\lambda$, where Δn is the birefringence. By linearizing Eq. (1), neglecting inertia, and solving for the rotational mean square displacement of a statistical ensemble of disks in the torque trap, we find:

$$\langle \Delta\theta_\alpha^2(t)\rangle = \frac{2k_{\text{B}}T}{\kappa}[1 - \exp(-\kappa t/\zeta)], \qquad (2)$$

where $\kappa = 2P_{\text{eff}}\sin(R)/\omega_o$ is the rotational spring constant due to the light torque, and k_{B} is Boltzmann's constant. This equation is the rotational counterpart to the translational harmonically bound Brownian particle [14]. At short times $t \ll \zeta/\kappa$, Eq. (1) simplifies to $\langle \Delta\theta_\alpha^2(t)\rangle = 2k_{\text{B}}Tt/\zeta$, indicating that diffusion dominates; the rotational diffusion coefficient is $\Theta = k_{\text{B}}T/\zeta$. However, at long times, $\langle \Delta\theta_\alpha^2(t)\rangle$ saturates to a constant, $\langle \Delta\theta_{\text{sat}}^2\rangle = 2k_{\text{B}}T/\kappa$, indicating that thermal energy is too small to rotate the disk out of the orientational trap. In Fig. 2(b), we fit the measured $\langle \Delta\theta_\alpha^2(t)\rangle$ to Eq. (2), and there is excellent agreement. The fit yields $\Theta = 6.7 \times 10^{-2}$ s^{-1}; this is close to $\Theta = 4.3 \times 10^{-2}$ s^{-1} predicted by Perrin's ellipsoid theory. The small error can be attributed to the difference in ζ between a disk and an ellipsoid and to the experimental uncertainty in a.

As shown in Fig. 3(a), the trapped disk can be spun on its edge by introducing a quarter wave plate above the dichroic mirror, changing the laser tweezer from LP to CP. This creates a driving radiation torque [10,11,15]:

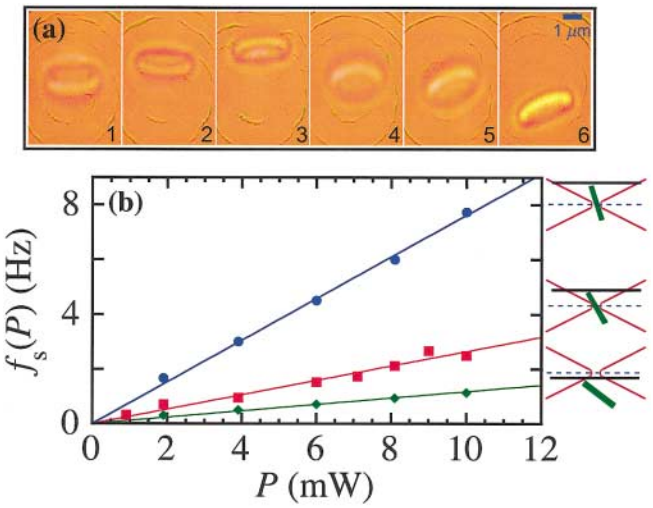

FIG. 4 (color). (a) Successive micrographs (1–6) separated by 1/6 s show the coupled translational-orientational switchback oscillation of the disk (radius 1.5 μm) in an LP laser tweezer ($P = 8$ mW) when the focal plane is 1 μm away from the slide. (b) Switchback oscillation frequency, f_s, as a function of laser power, P, for several different separations between the focal plane and glass slide: 1.4 μm (circles), 0.4 μm (squares), and -0.6 μm—slightly inside the slide wall—(diamonds). The frequency increases linearly with laser power, $f_s \sim P$ (solid line fits).

$\tau_{\text{rot}} = 2P_{\text{eff}} \sin^2(R/2)/\omega_o$. The light streaks rotate, forming a ''colloidal lighthouse'' with two flashes per period. The rotation frequency, f, grows linearly with P, as measured using an optical fiber connected to a photomultiplier tube [see Fig. 3(b)]. Using the higher power IR laser, trapped disks can be rotated rapidly with $f >$ 100 Hz. Adding a half wave plate changes the handedness of the circular polarization, and the disk rotates at the same rate in the opposite direction.

A confining wall significantly alters the stability of a disk in a LP tweezer. When a disk is moved upward and perturbed by the slide, the disk tilts and begins to translate in the direction perpendicular to the polarization direction. Gradients in the electric field and interaction with the wall cause the disk to rapidly tilt in the opposite direction and return back toward the center of the beam. This process repeats, creating the coupled translational-orientational ''switchback'' oscillation (SO) shown in Fig. 4(a). The SO frequency, f_s, is proportional to P and depends on the position of the focal plane relative to the glass surface [see Fig. 4(b)]. When the focal plane is near the glass slide, f_s becomes smaller due to increased viscous drag and to a small volume of the disk in the region of the highest electric field. The amplitude of the translational excursion and the tilt angle diminish as the distance between the slide and focal plane increases. Moving the focal plane well beyond the glass slide causes the SO to cease and the disk to lie flat against the slide. The SO can be explained by coupled force and torque equations that include, in addition to optical forces and torques, the effects of a normal force on the edge of the disk that is closest to the slide and a viscous drag torque (since the disk's edge closest to the slide experiences more resistance). Since the SO arises from the disk's anisotropic shape, it could not occur for trapped microspheres near a wall, but it might occur for other spatially anisotropic particles.

To determine which of the effects observed in the wax microdisks are due to anisotropy and which to birefringence, we have examined nonbirefringent PMMA disks of 2 μm diameter and 400 nm thickness [16]. We can stably trap the disks in the same edge-on configuration. However, even with the high power tweezer, we are neither able to arrest the rotational diffusion with LP light nor create the colloidal lighthouse effect with CP light. We conclude that the disk trapping and edge-on orientation result from the shape and the polarization effects are important only when the disk is birefringent.

In summary, we have presented the first studies of the interactions between laser tweezers and short cylindrical thin microdisks. A thin microdisk that has a thickness near or below the wavelength of light can be positionally trapped in 3D; it orients with its symmetry axis perpendicular to the beam's axis. This orientation produces forward and backscattered light streaks which serve as optical lever arms for sensitive detection of rotation. Birefringent microdisks can be spun on edge at high-speed using CP light, creating a colloidal lighthouse. We have shown that LST is an exciting new high-speed technique for measuring angular displacements of trapped disks, and we have used this technique to make the first detailed measurements of harmonically bound Brownian rotational motion of a birefringent colloidal disk in a LP optical trap. We have also discovered the instability and switchback oscillation of a trapped disk near a wall.

These discoveries open up new possibilities for positioning and orienting microdisks using laser tweezers. Birefringent disks, as with other recently reported micromachines [17,18], could be used in microfluidics mixers or to unwind DNA molecules. The light streak could be used in micro-optical routing and switching. Finally, an optically trapped microdisk could be used as a probe for studying biological or complex fluid rheology through rotational dynamics measured using LST.

We thank Matthew Sullivan for use of the IR laser tweezers, Christopher Harrison for his ''Tailored Colloids,'' and Yuexing Zhang for helpful discussions.

*Present address: DiCon Fiberoptics Inc., 1689 Regatta Blvd., Richmond, CA 94804.

[1] A. Ashkin, J. M. Dziedzic, J. E. Bjorkholm, and S. Chu, Opt. Lett. **11**, 288 (1986).
[2] T. T. Perkins, D. E. Smith, R. G. Larson, and S. Chu, Science **268**, 83 (1995).
[3] *Laser Tweezers in Cell Biology*, edited by M. P. Sheetz (Academic, San Diego, 1998).
[4] R. C. Gauthier, J. Opt. Soc. Am. B **14**, 3323 (1997).
[5] R. C. Gauthier, M. Ashman, and C. P. Grover, Appl. Opt. **38**, 4861 (1999).
[6] R. Bar-Ziv *et al.*, Phys. Rev. Lett. **78**, 154 (1997).
[7] A. Meller *et al.*, Biophys. J. **74**, 1541 (1998).
[8] H. Gang *et al.*, J. Phys. Chem. B **102**, 2754 (1998).
[9] S. Asakura and F. Oosawa, J. Chem. Phys. **22**, 1255 (1954).
[10] P. L. Maston and J. H. Crichton, Phys. Rev. E **30**, 2508 (1984).
[11] M. E. J. Friese, T. A. Nieminen, N. R. Heckenberg, and H. Rubinsztein-Dunlop, Nature (London) **394**, 348 (1998).
[12] E. Higurashi, R. Sawada, and T. Ito, Phys. Rev. E **59**, 3676 (1999).
[13] B. J. Berne and R. Pecora, *Dynamic Light Scattering with Applications to Chemistry, Biology, and Physics* (Dover, New York, 2000).
[14] T. G. Mason, H. Gang, and D. A. Weitz, J. Opt. Soc. Am. A **14**, 139 (1997).
[15] E. Higurashi, H. Tanaka, and O. Ohguchi, Appl. Phys. Lett. **64**, 2209 (1994).
[16] The PMMA disks were fabricated by Dr. Christopher Harrison using photolithography.
[17] P. Galajda and P. Ormos, Appl. Phys. Lett. **78**, 249 (2001).
[18] M. E. J. Friese, H. Rubinsztein-Dunlop, J. Gold, P. Hagberg, and D. Hanstorp, Appl. Phys. Lett. **78**, 547 (2001).